

# Resolving Systematic Errors in Sulfate Source Apportionment: A Field-Validated Kinetic Isotope Fractionation Framework

*Zhaobing Guo<sup>1,2</sup>, Xuexue Bai<sup>1</sup>, Qiwei Ai<sup>1</sup>, Zizheng Xu<sup>1</sup>, Shangshun Ma<sup>1</sup>, Jiayu Gu<sup>3</sup>,  
Pengxiang Qiu<sup>1\*</sup>, Qingjun Guo<sup>4\*</sup>*

<sup>1</sup>Jiangsu Key Laboratory of Atmospheric Environment Monitoring and Pollution Control (AEMPC), Collaborative Innovation Centre of Atmospheric Environment and Equipment Technology (CIC-AEET), School of Environmental Science and Engineering, Nanjing University of Information Science and Technology, Nanjing 210044, China

<sup>2</sup>Suqian University, Suqian 223800 China

<sup>3</sup>School of Chemical Engineering and Materials, Changzhou Institute of Technology, Changzhou 213032, China

<sup>4</sup>Center for Environmental Remediation, Institute of Geographic Sciences and Natural Resources Research, Chinese Academy of Sciences, Beijing 100101, China

## **Text S1. Estimation of primary sulfate and secondary sulfate**

The primary sulfate (calculated by  $0.18 \times \text{Ca}^{2+} + 0.25 \times \text{Na}^{+}$ )<sup>1</sup> contributed (2.65 ± 2.11% ) to total sulfate mass.

$$T_{PS} = T_{SS} + T_{ts} \quad (1)$$

$$T_{SS} = T_{bbus} + T_{cc} + T_{VS} + T_{os} \quad (2)$$

where  $T_{PS}$ ,  $T_{SS}$ ,  $T_{ts}$ ,  $T_{SS}$ ,  $T_{bbus}$ ,  $T_{cc}$ ,  $T_{vs}$ ,  $T_{os}$  are the primary sulfate (ps), sea salt sulfate (ss), terrestrial sulfate (ts), secondary sulfate(SS),biomass burning sulfate (bbus), coal combustion(cc), vehich sulfate(vs),oil sulfate(os).

### **Text S2. Calculation of $^{34}\text{S}$ Fractionation.**

Theoretical  $\delta^{34}\text{S-SO}_4^{2-}$  values can be calculated using the following equation according to previous studies<sup>2-4</sup>:

$$\delta^{34}\text{S} - \text{SO}_4^{2-} \textit{theoretical} = \sum \delta^{34}\text{S} - \varepsilon_i \times \ln(1 - \text{SOR}) \times (1 - \text{SOR})/\text{SOR} \quad (3)$$

where  $\sum \delta^{34}\text{S}$  is calculated using eq 4;  $\varepsilon_i$  is the  $\delta^{34}\text{S}$  fractionation factor between gas-phase  $\text{SO}_2$  and particulate  $\text{SO}_4^{2-}$  generatedthrough different  $\text{SO}_4^{2-}$  formation pathways ; and SOR is the ratio of  $\text{SO}_4^{2-}$  to  $(\text{SO}_4^{2-} + \text{SO}_2)$ , which ranges from 0 to 1.

$$\sum \delta^{34}\text{S} = \frac{[\text{SO}_2] \times \delta^{34}\text{S} - \text{SO}_2 + [\text{SO}_4^{2-}] \times \delta^{34}\text{S} - \text{SO}_4^{2-}}{[\text{SO}_2] + [\text{SO}_4^{2-}]} \quad (4)$$

where  $[\text{SO}_2]$  and  $[\text{SO}_4^{2-}]$  are the concentrations of gas-phase  $\text{SO}_2$  and particulate  $\text{SO}_4^{2-}$  in the atmosphere, respectively;  $\delta^{34}\text{S-SO}_2$  is the gas-phase  $\text{SO}_2$  value, and  $\delta^{34}\text{S-SO}_4^{2-}$  is the  $\delta^{34}\text{S-SO}_4^{2-}$  value in  $\text{PM}_{2.5}$  in Nanjing.

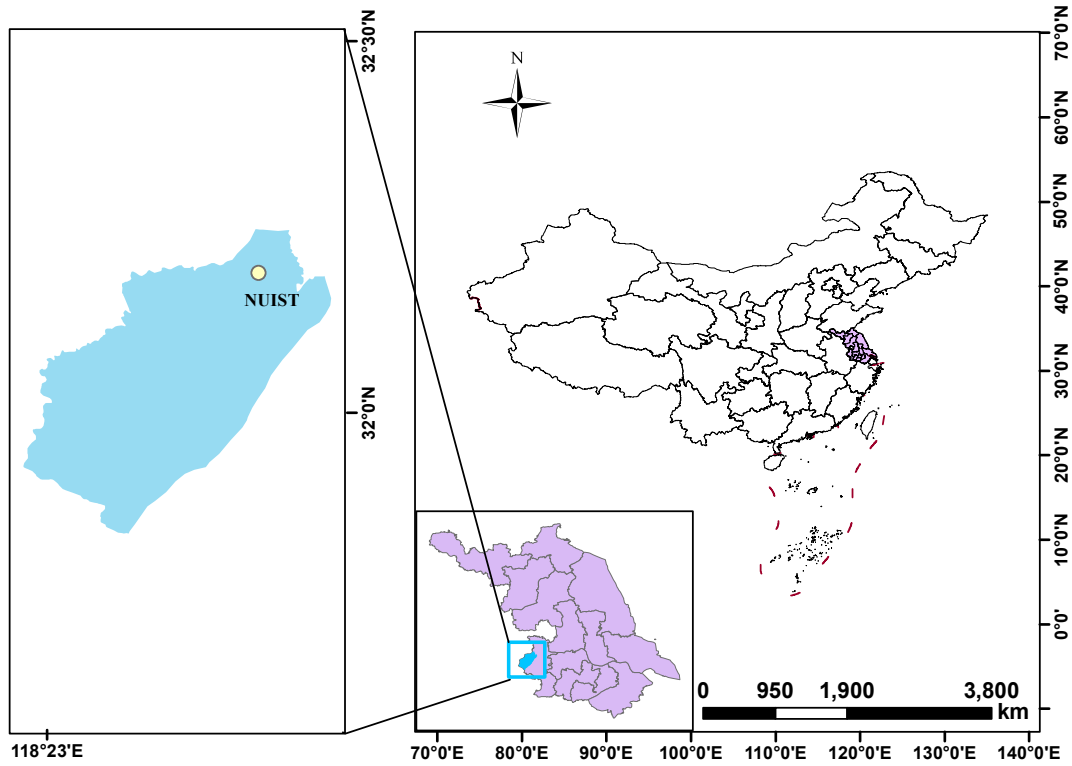


**Figure S1.** Map of atmospheric PM<sub>2.5</sub> sampling site in Nanjing City.

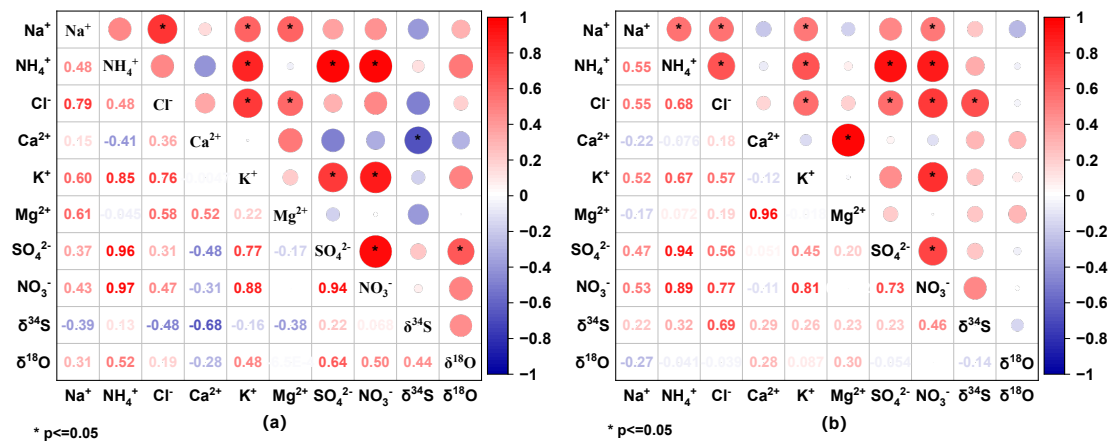


**Figure S2.** Correlation coefficients of water-soluble ions and stable isotopes in PM<sub>2.5</sub> in Nanjing (a: winter b: Summer).

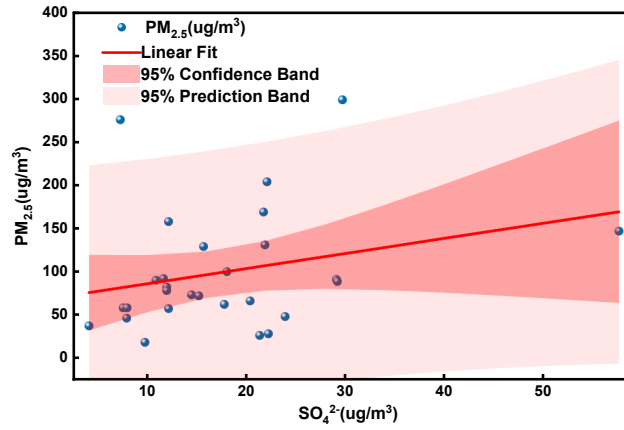


**Figure S3.** Scatter plot of  $\text{SO}_4^{2-}$  in  $\text{PM}_{2.5}$  in Nanjing.

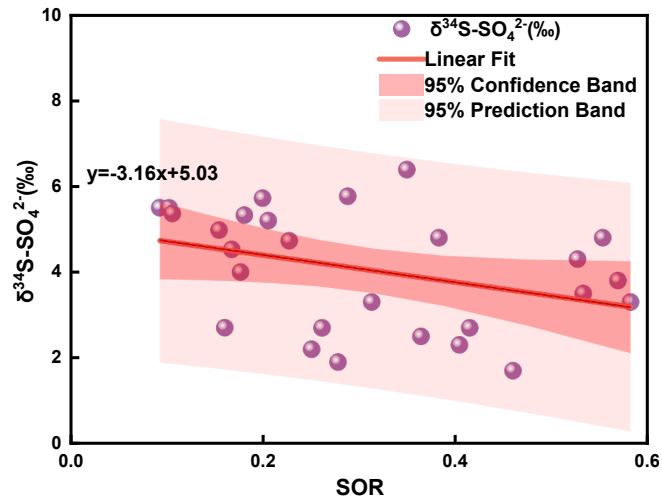


**Figure S4.** Scatter plot of  $\delta^{34}\text{S-SO}_4^{2-}$  values against SOR in Nanjing during the sampling period.

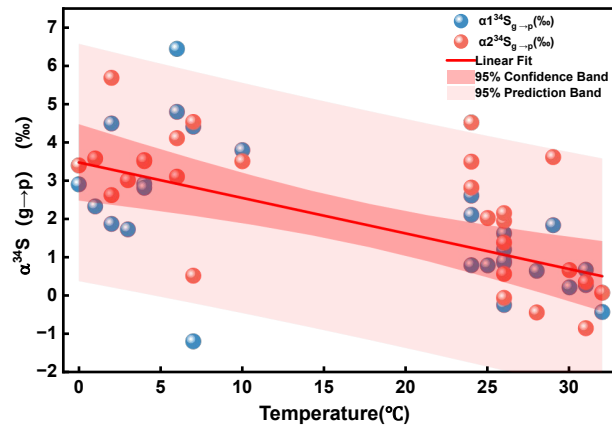


**Figure S5.** Scatter plot of  $\alpha^{34}\text{S}_{\text{g}\rightarrow\text{p}}$  against the ambient temperature in Nanjing during the sampling period.

**Table S1.** The  $\delta^{34}\text{S}$ - $\text{SO}_2$  values of various Chinese emission sources used in this study.

Source	$\delta^{34}\text{S}(\text{‰})$	Reference
Coal combustion	$4.6\pm 2.7$	Zheng et al. <sup>6</sup> Zhang et al. <sup>17</sup> Wei et al. <sup>18</sup>
Traffic emission	$6.6\pm 2.1$	Wei et al. <sup>18</sup> Feng et al. <sup>19</sup>
Biomass burning	$7.2\pm 1.5$	Fan et al. <sup>1</sup> Wei et al. <sup>18</sup> Guo et al. <sup>20</sup>
Oil combustion	$6.5\pm 2.4$	Zheng et al. <sup>6</sup> Wei et al. <sup>18</sup> Guo et al. <sup>20</sup>

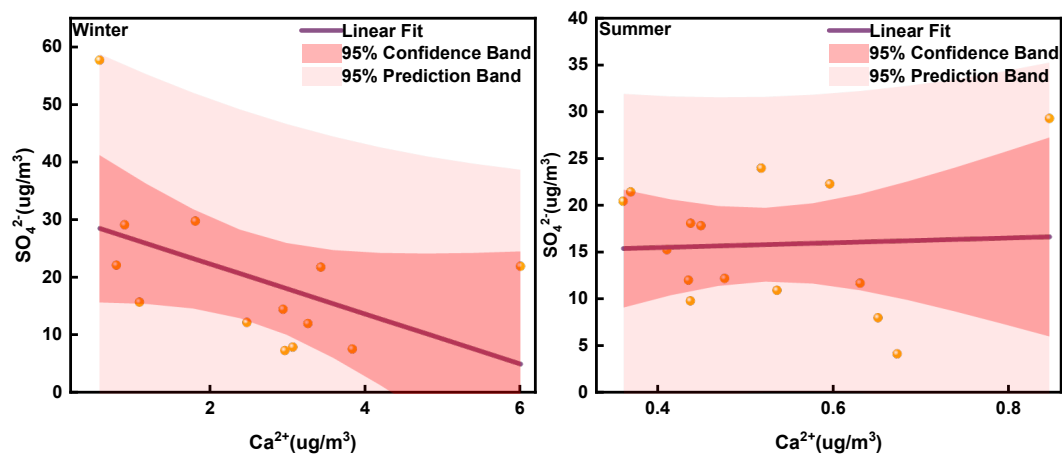


**Figure S6.** Scatter plot of  $\text{SO}_4^{2-}$  versus  $\text{Ca}^{2+}$  in  $\text{PM}_{2.5}$  during the sampling periods in Nanjing during the sampling period.

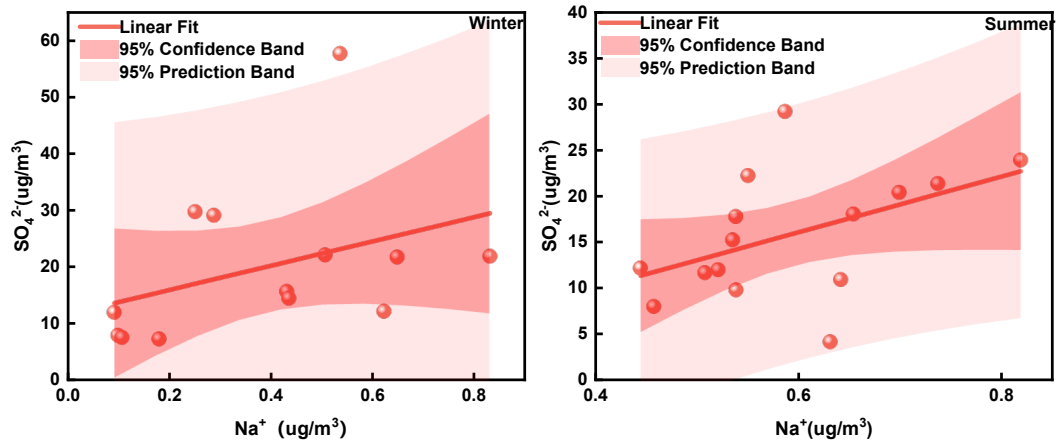


**Figure S7.** Scatter plot of  $\text{SO}_4^{2-}$  versus  $\text{Na}^+$  in  $\text{PM}_{2.5}$  during the sampling periods in Nanjing during the sampling period.

## REFERENCES

- (1) Fan, M.; Zhang, Y.; Lin, Y.; Li, J.; Cheng, H.; An, N.; Sun, Y.; Qiu, Y.; Cao, F.; Fu, P. Roles of sulfur oxidation pathways in the variability in stable sulfur isotopic composition of sulfate aerosols at an Urban Site in Beijing, China. *Environ. Sci. Technol. Lett.* **2020**, 7 (12), 883-888. DOI: 10.1021/acs.estlett.0c00623
- (2) Li, J.; Zhang, Y.; Cao, F.; Zhang, W.; Fan, M.; Lee, X.; Michalski, G. Stable sulfur isotopes revealed a major role of transition-metal ion-catalyzed SO<sub>2</sub> oxidation in haze episodes. *Environ. Sci. Technol.* **2020**, 54 (5), 2626-2634. DOI: 10.1021/acs.est.9b07150
- (3) Lin, M.; Zhang, X.; Li, M.; Xu, Y.; Zhang, Z.; Tao, J.; Su, B.; Liu, L.; Shen, Y.; Thiemens, M. H. Five-S-isotope evidence of two distinct mass-independent sulfur isotope effects and implications for the modern and Archean atmospheres. *Proc. Natl. Acad. Sci. USA* **2018**, 115 (34), 8541-8546. DOI:10.1073/pnas.1803420115
- (4) Yang, R.; Lou, Q.; Wang, M.; Cao, L.; Luo, L. Using stable sulfur isotopes to quantify the formation mechanism and sources of SO<sub>4</sub><sup>2-</sup> in PM<sub>2.5</sub> in Haikou city. *ACS Earth Space Chem.* **2025**, 9 (3), 560-568. DOI: 10.1021/acsearthspacechem.4c00304
- (5) Lin, Y.; Yu, M.; Xie, F.; Zhang, Y. Anthropogenic emission sources of sulfate aerosols in Hangzhou, East China: Insights from isotope techniques with consideration of fractionation effects between gas-to-particle transformations. *Environ. Sci. Technol.* **2022**, 56 (7), 3905-3914. DOI: 10.1021/acs.est.1c05823

(6) Zheng, M.; Song, D.; Zhang, D.; Cao, Y.; Fan, H. Using sulfur isotopes to constrain the sources of sulfate in PM<sub>2.5</sub> during the winter in Jiaozuo City. *Atmos. Environ.* **2024**, 332, 120618. DOI:10.1016/j.atmosenv.2024.120618

(7) Lin, Y. C.; Fan, M. Y.; Yu, M.; Abulimiti, A.; Xie, F.; Xu, R.; Zhang, Y. L. Significant contributions of regional transport to sulfate aerosols during haze events in Northern China Plain: Constrained by sulfur isotopic compositions. *J. Geophys. Res. Atmos.* **2025**, 130, e2025JD043716. DOI: 10.1029/2025JD043716

(8) Akata, N.; Yanagisawa, F.; Kotani, T. et al. Ten-year observation of sulfur isotopic composition of sulfate in aerosols collected at Tsuruoka, a coastal area on the Sea of Japan in northern Japan. *Geochem. J.* **2013**, 44(6), 571-577. DOI:10.2343/geochemj.1.0099

(9) Sakata, M.; Ishikawa, T.; Mitsunobu, S. Effectiveness of sulfur and boron isotopes in aerosols as tracers of emissions from coal burning in Asian continent. *Atmos. Environ.* **2013**, 67(MAR.), 296-303. DOI:10.1016/j.atmosenv.2012.11.025

(10) Saltzman, E. S.; Brass, G. W.; Price, D. A. et al. The mechanism of sulfate aerosol formation: Chemical and sulfur isotopic evidence. *Geophys. Res. Lett.* **1983**. DOI:10.1029/GL010i007p00513.

(11) Agnihotri, R.; Karapurkar, S. G.; Sarma, V. V. S. S. et al. Stable Isotopic and chemical characteristics of bulk aerosols during winter and summer season at a station in western coast of India (Goa). *Aerosol Air Qual. Res.* **2015**, 15(3), 888-900. DOI:10.4209/aaqr.2014.0

- (12) Li, J.; Michalski, G.; Davy, P. et al. Investigating source contributions of size-aggregated aerosols collected in southern ocean and baring head, New Zealand using sulfur isotopes. *Geophys. Res. Lett.* **2018**. DOI:10.1002/2018GL077353
- (13) Proemse, B. C.; Mayer, B.; Chow, J. C. et al. Isotopic characterization of nitrate, ammonium and sulfate in stack PM<sub>2.5</sub> emissions in the Athabasca Oil Sands Region, Alberta, Canada. *Atmos. Environ.* **2012**, 60(DEC.), 555-563. DOI:10.1016/j.atmosenv.2012.06.046
- (14) Calhoun, J. A.; Bates, T. S.; Charlson, R. J. Sulfur isotope measurements of submicrometer sulfate aerosol particles over the Pacific Ocean. *Geophys. Res. Lett.* **2013**, 18(10), 1877-1880. DOI:10.1029/91GL02304
- (15) Ishino, S.; Hattori, S.; Savarino, J. et al. Homogeneous sulfur isotope signature in East Antarctica and implication for sulfur source shifts through the last glacial-interglacial cycle. *Sci. Rep.* **2019**, 9(1), 1-8. DOI:10.1038/s41598-019-48801-1
- (16) Ghahremaninezhad, R.; Norman, A. L.; Abbatt, J. P. D. et al. Biogenic, anthropogenic and sea salt sulfate size-segregated aerosols in the Arctic summer. *Atmos. Chem. Phys.* **2016**, 16(8), 5191-5202. DOI:10.5194/acp-16-5191-2016
- (17) Zhang, H.; Hu, A.; Lu, C.; Zhang, G. Sulfur isotopic composition of acid deposition in South China Regions and its environmental significance. *China Environ. Sci.* **2002**, 22 (2), 165-169. DOI: 10.3321/j.issn:1000-6923.2002.02.01

(18) Wei, Y.; Guo, Z.; Ge, X. et.al. Tracing sources of sulfate aerosol in Nanjing northern suburb using sulfur and oxygen isotopes. *Chin. J. Environ. Sci* **2015**, *36* (4), 1182-1186. DOI: 10.13227/j.hjkx.2015.04.006

(19) Feng, X.; Chen, Y.; Liu, Z.; Feng, Y.; Du, H.; Mu, Y.; Chen, J.. Exploring the influence of  $^{34}\text{S}$  fractionation from emission sources and  $\text{SO}_2$  atmospheric oxidation on sulfate source apportionment based on hourly resolution  $\delta^{34}\text{S}\text{-SO}_2/\text{SO}_4^{2-}$ . *J. Geophys. Res. Atmos.* **2023**, *128*, e2023JD038595. DOI: 10.1029/2023JD038595

(20) Guo, Z.; Shi L.; Chen S.; Jiang W.; Wei Y.; Rui M.; Zeng G. Sulfur isotopic fractionation and source appointment of  $\text{PM}_{2.5}$  in Nanjing region around the second session of the Youth Olympic Games. *Atmos. Res.* **2016**, *174-175*, 9-17. DOI: 10.1016/j.atmosres.2016.01.011.